**Room Temperature Magnetic Quantum Cellular Automata**

R. P. Cowburn and M. E. Welland

*Processing and Properties of Nanocrystalline Materials*, C. Suryanarayana, J. Singh, F. H. Froes, Eds. (TMS, Warrendale, PA, 1996), p. 379.

9. N. Wang, Z. R. Wang, K. Aust, U. Erb, *Mater. Sci. Eng.* **A237**, 150 (1997).
10. P. G. Sanders *et al.*, *Nanostruct. Mater.* **9**, 433 (1997).
11. S. X. McFadden *et al.*, *Nature* **398**, 684 (1999).
12. U. Erb, A. M. El-Sherik, G. Palumbo, K. T. Aust, *Nanostruct. Mater.* **2**, 383 (1993).
13. H. P. Klug and L. E. Alexander, *X-Ray Diffraction Procedures for Polycrystalline and Amorphous Materials* (Wiley, New York, 1974), p. 618.
14. R. S. Mishra, S. X. McFadden, A. K. Mukherjee, *Mater. Sci. Forum Vols.* **304**, 31 (1999).
15. B. Cai, Q. P. Kong, L. Lu, K. Lu, *Scr. Metall.* **41**, 755 (1999).
16. J. Horvath, R. Birringer, H. Gleiter, *Solid State Comm.* **62**, 391 (1987).
17. H. Hahn, P. Mondal, K. A. Padmanabhan, *Nanostruct. Mater.* **9**, 603 (1997).
18. Supported by the Chinese Academy of Sciences, the National Science Foundation of China (grants 59431021 and 59625101), and the Ministry of Sciences and Technology of China (grant G1999064505). The authors thank S. L. Gu for his assistance in sample preparation.

13 October 1999; accepted 21 December 1999

# Room Temperature Magnetic Quantum Cellular Automata

R. P. Cowburn* and M. E. Welland

**All computers process information electronically. A processing method based on magnetism is reported here, in which networks of interacting submicrometer magnetic dots are used to perform logic operations and propagate information at room temperature. The logic states are signaled by the magnetization direction of the single-domain magnetic dots; the dots couple to their nearest neighbors through magnetostatic interactions. Magnetic solitons carry information through the networks, and an applied oscillating magnetic field feeds energy into the system and serves as a clock. These networks offer a several thousandfold increase in integration density and a hundredfold reduction in power dissipation over current microelectronic technology.**

The silicon microchip has been one of the most impressive feats of engineering ever performed. In the case of microprocessors, the number of transistors on a chip has steadily doubled every 18 months for the last 25 years, with a commensurate growth in information-processing capability (*1*). While there is still much potential for future growth, a point will eventually come when further increases become prohibitively difficult (*2*). At this point there may be interest in introducing a new paradigm for digital logic. Much interest has recently been focused on single electron transistors (SETs) as candidates for continuing the growth of both processors and memory beyond that of conventional silicon devices (*3*). A particularly interesting configuration of SETs called quantum cellular automata (QCA) has recently shown the ability to perform logic operations (*4*). Unfortunately, these devices only work at very low temperatures (millikelvin) unless the SET island dots are made to be extremely small (~2 nm).

We demonstrate experimentally that QCA architectures using relatively large dots (~100 nm) can be made to work at room temperature if one uses magnetic metals to make the dots.

Each QCA network (Fig. 1) consists of a single elongated input dot followed by a chain of 69 circular dots, each of diameter 110 nm, placed on a pitch of 135 nm. The dots were 10 nm thick and were made from the common magnetic alloy Supermalloy ($Ni_{80}Fe_{14}Mo_5X_1$, where X is other metals) on a single-crystal silicon substrate. The uniaxial anisotropy field in the unpatterned Supermalloy was less than 3 Oe. The dots were fabricated by high-resolution electron beam lithography in a polymethlymethacrylate resist followed by metalization and ultrasonic assisted lift-off in acetone. Further technical details of the fabrication and structural characterization of our magnetic nanostructures can be found in (*5*).

Electronic QCA is termed "quantum" because it uses quantum mechanical tunneling of charge between dots to change logic state; classical electrostatics are used thereafter to propagate the logic state. The quantum mechanical interactions in the magnetic QCA (MQCA) networks are exchange interactions between spins within a single dot in order to form a single giant classical spin (*5*). A logic 1 is signaled when the dot's magnetization vector points to the right, say, and a logic 0 when it points to the left. The magnetic field emanating from such a magnetic particle can be extremely large, with the result that one magnetic dot is strongly influenced by the magnetic field coming from its nearest neighbors. These classical magnetostatic interactions are then used to propagate information along the chain of dots (*6*). A further feature of magnetostatic interactions is that they force the magnetization to point along the length of the chain. The system is thus intrinsically binary, with only right- and left-pointing magnetization states being stable.

Elongating the shape of a dot introduces shape anisotropy, which greatly increases its switching field. Such a dot is still able to influence neighboring circular dots but is itself unaffected by them. We therefore use elongated dots to inject signals into the network. We set the state of the input dots by an external pulsed magnetic field applied to the entire network. Once set, the shape anisotropy of the input dots ensures that their magnetization state is preserved until the next field pulse.

We choose for simplicity to probe the magnetic state of the MQCA networks by a magneto-optical measurement (*7*). A linearly polarized laser beam is focused onto the networks, and the polarization state of the reflected light is measured in order to access the longitudinal Kerr effect (*8*). The plane of incidence of the light is set to lie along the length of the chains. The focused laser spot covers almost the entire 9-μm length of the networks, and so the recorded signal is a measure of the total component of magnetization lying along the chain of dots and, once
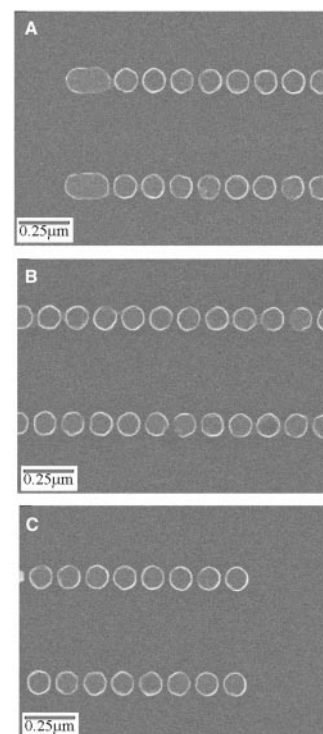


**Fig. 1.** Scanning electron micrographs of the left (**A**), center (**B**), and right (**C**) regions of two of the room temperature MQCA networks that we have fabricated.

Nanoscale Science Laboratory, Department of Engineering, University of Cambridge, Trumpington Street, Cambridge CB2 1PZ, UK.

*To whom correspondence should be addressed. E-mail: rpc12@cam.ac.uk

correctly calibrated, is a measure of the number of dots switching in a network. The signal-to-noise statistics were improved and the repeatability of any effects tested by fabricating 20 networks together (separated by 0.5 μm; Fig. 1 shows 2 of the 20 networks) and measuring the total resulting signal, averaged over 2 min of acquisition time. The 0.5-μm separation is easily sufficient to isolate the networks from each other magnetically.

The input dots are set by applying a single magnetic field pulse (using remanence-free Helmholtz coils) of either +300 Oe (for a logic 1) or −300 Oe (for a logic 0) directed along the chain of dots, returning to 0 Oe at the end of the pulse. A weak oscillating magnetic field of ±25-Oe amplitude and 30-Hz frequency combined with a −10-Oe bias magnetic field is then applied along the chain of dots. The magneto-optical signal from the networks is recorded over several cycles (Fig. 2). When the input dots are set to 0 (magnetization points to the left), no response is observed; when the input dots are set to 1 (magnetization points to the right), all of the networks switch in step with the applied oscillating field. If one assigns the negative phase of the oscillating field to a logic 0 and the positive phase to a logic 1, then the response of the networks is the logical AND of the input dot with the oscillating field. The scale of Fig. 2 is calibrated in number of dots switching within each network. The fact that the signal in Fig. 2C has an amplitude of ~±60 shows that almost the entire chain of 69 dots is switching. In other words, the

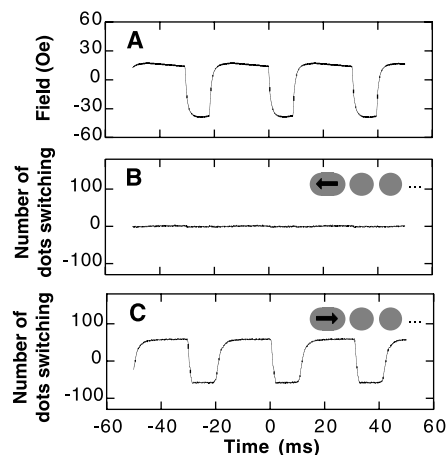magnetization direction of the single input dot determines the magnetic state of 69 other dots. Signal propagation along the length of the chain is thus clearly occurring.

To confirm that the effect is not due to some memory of the pulsed field (used to set the input dots) residing in the circular dots, we performed an identical experiment on control networks in which the elongated input dots were absent (Fig. 3). Even though the input magnetizing field pulses are still applied, no response is observed in either case. The difference between the signals of Fig. 2, B and C, must therefore be due to the presence of the input dots.

The device operates in the following way. The easiest way to reverse the magnetic state of the chain of dots is to propagate a magnetic soliton along it. The soliton is analogous to a domain wall in a bulk magnetic material and separates regions of left magnetization from right magnetization (Fig. 4A). Being a topological object, the soliton must be explicitly created somewhere; the most probable creation site is at the far right-hand end of the chains where there is only one nearest neighbor dot. Although soliton creation is a highly energetic process, the soliton, once created, can propagate along the chain under relatively weak fields (because the dots at the center of the soliton—P and Q in Fig. 4A—experience zero net interaction field and so can be reversed easily, moving the soliton on by one step).

The combination of the bias and oscillating fields means that during the negative phase of the oscillation, a strong enough field is applied to create a soliton at the right-hand end of the chain and then propagate it, setting
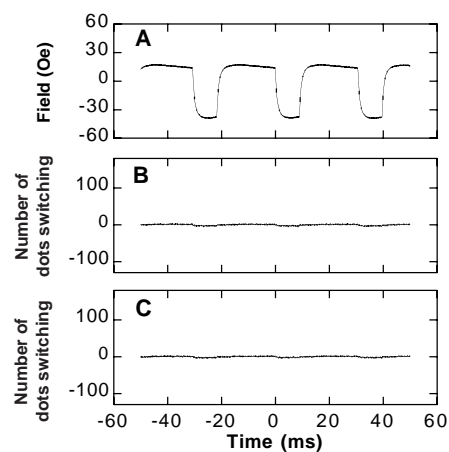
all of the circular dots to state 0. However, the fields are not strong enough to switch the input dots. If the input dot is set to 0, then the entire chain is now in the 0 state (Fig. 4B). When the oscillating field subsequently enters its positive phase, the net field, being only weakly positive, is unable to create a new soliton. The network therefore cannot switch and remains permanently in the 0 state (Fig. 2B). If, on the other hand, the input dot is set to 1, then at the end of the negative phase of the oscillating field a soliton already exists between the input dot and the most leftward circular dot (Fig. 4C). As the oscillating field enters its positive phase, the soliton is propagated to the right and switches the chain to the 1 state. The entire chain thus switches in step with the applied oscillating field (Fig. 2C). We have performed Monte Carlo numerical simulations of the network to verify that this qualitative description is indeed correct.

We have chosen a very simple MQCA network as proof of the principle that logic operations and information propagation can be performed at room temperature. In this particular network, the first circular dot acts as an AND gate with the oscillating clock field as one input and the elongated dot as the other input. Circular dots 2 to 69 act as output interconnect. Preliminary Monte Carlo simulations indicate that much more complex networks will also work. The magnetostatic interaction field between two of the neighboring dots is ~50 Oe, which is comparable in strength to the bias and clock fields. Further dots could therefore be added to provide additional inputs or local biases, allowing a variety of logic functions between several locally applied signals to be performed. By changing the direction of the applied clock field such that there is a component in both
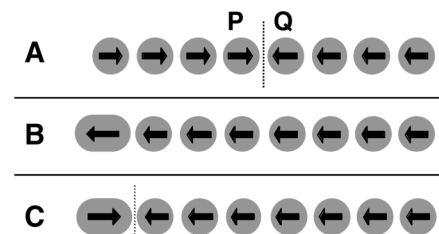
**Fig. 2.** Room temperature experimental results from the MQCA networks shown in Fig. 1. (**A**) The combined applied oscillating and bias fields; (**B**) the magneto-optical response of the MQCA networks for the case of the input dots set to 0 and (**C**) for the input dots set to 1, calibrated in number of dots switching within one network. The width of the edge transitions in (C) is not due to the temporal response of the MQCA networks but rather to a small distribution in switching fields, combined with the finite switching time of the applied oscillating field.



**Fig. 3.** (**A** to **C**) The results of the experiment reported in Fig. 2 performed on control networks in which the input dots were absent. To within experimental error, there is no response. The very faint signal seen in (B) and (C) can be explained as a ±1.5° rotation of the magnetization with the oscillating field as a result of a systematic misalignment (±2°) of the applied field with the axis of the chains.



**Fig. 4.** A schematic of the vector magnetization (arrows) in a number of dots. (**A**) A soliton in the center of a chain of circular dots. The center of the soliton is between dots P and Q. The magnetic state of the network at the end of the negative phase of the applied oscillating field is shown for the cases of the input dot set to 0 (**B**) and the input dot set to 1 (**C**). The center of the solitons is marked by a dashed line. Micromagnetic calculations show that the precise soliton structure is not quite as abrupt as shown here, but that small oscillations in magnetization direction continue for a small number of dots on either side of the soliton center.

the $x$ and $y$ directions of the network of dots, solitons can be propagated along chains that turn corners. There is, in principle, no physical problem in splitting a soliton into two channels, and so fan-out of signals should also be possible. Further simulations show that NOT functions, concatenated gates, and crossing chains are also possible [see (9) for electronic QCA implementations]. The fact that they operate at room temperature and are fabricated from a size of dot that could be manufactured commercially makes them ideal candidates for integration into microelectronic hardware. Input dots could be programmed locally by passing an electrical current through a conducting track underneath the dot, as in magnetic random access memory (10, 11). Signal output could be obtained from single dots in a complex network by using one of the recently discovered magnetoelectronic effects (10).

Power gain is a very important issue in all QCA architectures. Electronic QCA circumvents this by temporarily removing the energy barriers between logic states during switching, to allow near-adiabatic operation (12). In principle, MQCA solitons propagate without loss and so should be able to mediate a logic switch without any dissipation; in practice, small fluctuations in the shape of the dots will lead to anisotropy fluctuations (the size of dots reported here gain ~10 Oe of anisotropy field for each percent of ellipticity in shape), which will cause the soliton to dissipate energy as it propagates. In our MQCA architecture, this energy is provided by the externally applied oscillating magnetic field. Power gain to overcome losses and to enable fan-out of signals can thus be achieved.

The need to minimize anisotropy fluctuations places a required accuracy on the circularity of the dots of better than $\pm 2\%$. We can infer from the signal level of Fig. 2C that this accuracy has been achieved in at least 19 of the 20 networks that we fabricated using only conventional electron beam lithography. Furthermore, this fabrication requirement is one order of magnitude less stringent than that of electronic QCA (13).

MQCA has enormous potential to meet the future requirements of microelectronics for digital processing. If we take a single MQCA dot to be analogous to a transistor (comparing different paradigms is difficult, but this allows for an order of magnitude comparison), then the unoptimized device we report here has an integration density of 5500 million $cm^{-2}$, compared with 6.6 million $cm^{-2}$ for today's CMOS technology (14). The magnetostatic interaction energy between two of the dots reported here is 200 $k_B T$ ($k_B$ is Boltzmann's constant and $T$ is room temperature). An energy of at least 40 $k_B T$ is required if thermally induced data errors are to be kept below one per year. MQCA should therefore be very stable against thermal fluctuations. Simple scaling laws show that this will remain the case for dots as small as 20 nm in diameter, giving a possible integration density of 250,000 million $cm^{-2}$. The maximum energy that any magnetic object of volume $V$ can dissipate in one field cycle of peak-to-peak amplitude $H$ is $8\pi M_s HV$ ($M_s$ is the saturation magnetization in centimeter-gram-second units), which gives a maximum dot dissipation of $10^{-17}$ J per clock cycle (for the size of dots described here). This is $10^4$ times less than the power-delay product of $10^{-13}$ J for today's CMOS (15), meaning that a microprocessor based on MQCA would typically dissipate around only 1 W. Recent studies (16) have shown that submicrometer magnetic particles can be switched in less than 1 ns. This gives a conservative estimate on the order of 100 MHz for the maximum expected across-chip clock frequency of MQCA devices, although full dynamic calculations and experiments will be essential to determine the influence of spin-wave excitations. The fact that entire networks can be constructed on a single plane means that many planes could in principle be stacked on top of each other, thus giving a way to realize three-dimensional hardware.

**References and Notes**
1. R. R. Schaller, *IEEE Spectrum* **34** (no. 6), 52 (1997).
2. M. Schulz, *Nature* **399**, 729 (1999).
3. H. Ahmed and K. Nakazato, *Microelectron. Eng.* **32**, 297 (1996); K. K. Likharev, *Proc. IEEE* **87**, 606 (1999).
4. I. Amlani *et al.*, *Science* **284**, 289 (1999).
5. R. P. Cowburn, D. K. Koltsov, A. O. Adeyeye, M. E. Welland, D. M. Tricker, *Phys. Rev. Lett.* **83**, 1042 (1999).
6. R. P. Cowburn, A. O. Adeyeye, M. E. Welland, *N. J. Phys.* **1**, 16 (1999).
7. R. P. Cowburn, D. K. Koltsov, A. O. Adeyeye, M. E. Welland, *Appl. Phys. Lett.* **73**, 3947 (1998).
8. A. Hubert and R. Schäfer, in *Magnetic Domains: The Analysis of Magnetic Microstructure* (Springer, Berlin, 1998), p. 24.
9. W. Porod *et al.*, *Int. J. Electron.* **86**, 549 (1999).
10. W. J. Gallagher *et al.*, U.S. Patent 5 640 343 (1997).
11. G. A. Prinz, *Science* **283**, 5400 (1999).
12. C. S. Lent and P. D. Tougaw, *Proc. IEEE* **85**, 541 (1997).
13. C. G. Smith, *Science* **284**, 274 (1999).
14. Semiconductor Industry Association International Technology Roadmap for Semiconductors 1999 (Sematech, Austin, TX, 1999); www.sematech.org
15. R. Compañó, L. Molenkamp, D. J. Paul, *Technology Roadmap for European Nanoelectronics* (1999), p. 12.
16. R. L. Stamps and B. Hillebrands *Appl. Phys. Lett.* **75**, 1143 (1999); A. V. Pohm, J. M. Anderson, R. S. Beech, J. M. Daughton, *J. Appl. Phys.* **85**, 4771 (1999); S. E. Russek, J. O. Oti, S. Kaka, E. Y. Chen, *J. Appl. Phys.* **85**, 4773 (1999).
17. R.P.C. was supported by St. John's College, Cambridge.

11 November 1999; accepted 18 January 2000

# Rippling Instability of a Collapsing Bubble

**Rava da Silveira,[1] Sahraoui Chaïeb,[2] L. Mahadevan[2]**

When a bubble of air rises to the top of a highly viscous liquid, it forms a dome-shaped protuberance on the free surface. Unlike a soap bubble, it bursts so slowly as to collapse under its own weight simultaneously, and folds into a wavy structure. This rippling effect occurs for both elastic and viscous sheets, and a theory for its onset is formulated. The growth of the corrugation is governed by the competition between gravitational and bending (shearing) forces and is exhibited for a range of densities, stiffnesses (viscosities), and sizes—a result that arises less from dynamics than from geometry, suggesting a wide validity. A quantitative expression for the number of ripples is presented, together with experimental results that support the theoretical predictions.

Every day, nature surprises us with structures and patterns of such beauty as to fill the scientist with wonder and the artist with envy. Here, we address an instability that turns a hemispherical, smooth, liquid bubble into a striking wrinkled structure, first observed by Debrégeas, de Gennes, and Brochard-Wyart (1). In their experiment, 0.1 to 10 $cm^3$ of air injected into a highly viscous liquid (with viscosity $\eta \sim 10^3$ Pa·s) rises to the free surface, imprisoned in a hemispherical bubble of thickness $t \sim 1$ to 10 $\mu$m. If the bubble is punctured at its apex by a needle, surface tension drives the rapid expansion of a circular opening. After about 10 to 30 ms, the retraction velocity saturates to a constant, owing to the high viscous resistance. In the meantime, the air flow through the hole equilibrates the pressure difference, allowing the bubble to collapse under its own weight. As it deflates, an instability appears: The fluid sheet folds into a wavy structure, with radial ripples that break the original axisymmetry. In the absence of a detailed theory, a scaling estimate has been proposed (1) for the number of ripples: $n^* \sim (\mu g R^3/K)^{1/2}$, where $\mu$ is the mass of the film per unit area, $g$ is the gravitational acceleration, $R$ is the radius of the hole, and $K$ is an effective bending rigidity of the sheet (which was assumed to be

[1]Department of Physics, [2]Department of Mechanical Engineering, Massachusetts Institute of Technology, Cambridge, MA 02139, USA.